Food & Health 2020, 3(4): 7-13

Food & Health
Journal homepage: fh.srbiau.ac.ir
Journal

Performance of machine learning system to prediction of almond physical properties

Mohsen Mokhtarian [1*], Hamid Tavakolipour [2], Hassan Hamedi [3], Amir Daraei Garmakhany [4]

[1] Department of Food Science and Technology, Roudehen Branch, Islamic Azad University, Roudehen, Iran
[2] Department of Food Science and Technology, Sabzevar Branch, Islamic Azad University, Sabzevar, Iran
[3] Department of Food Safety and Hygiene, Science and Research Branch, Islamic Azad University, Tehran, Iran
[4] Department of Food Science and Technology, Tuyserkan Faculty of Engineering & Natural Resources, Bu-Ali Sina University, Hamedan, Iran.

A R T I C L E I N F O

Original Article

Article history:
Received 12 September 2020
Revised 21 October 2020
Accepted 22 November 2020
Available online 20 December 2020

Keywords:
Artificial neural network
Almond
Axial dimensions
Engineering properties

A B S T R A C T

The physical properties of almond kernel are necessary for the proper design of equipment for transporting, drying, processing, sorting, grading, and storage this crop. In this study, different models of ANNs with different activation functions were used to forecast surface area, volume, mass, and kernel density of almond. The results showed that multilayer perceptron network with tanh-tanh activation function as a goodness activation function can be estimated surface area, volume, mass, and kernel density with R2 value 0.983, 0.986, 0.981, and 0.982, respectively. Furthermore, the physical properties were fitted by regression relationships, the result showed linear regression method can be predicted surface area, volume, mass and kernel density with R2 value 0.979, 0.961, 0.945, and 0.791, respectively. Generally, the result showed neural network model had high ability to forecast the physical properties of almond than the linear regression method.

1. Introduction

Almond (*Amygdales Communist* L.) is a dried fruit widely used, especially in the food industry. The almond kernels form an important source of energy with 6 kcal/g, protein 15.64%, and their oil content changed from 35.27% to 40% (1). Physical properties of agricultural materials affect how they are to be processed, handled, stored, and consumed and so are required in the design of planting, harvesting, and post-harvest operations such as cleaning, conveying, and storage (2). Presently, all the post-harvest handling and processing practices are done manually and it is necessary to design tools, equipment, and machines for these processes. However, before the design and fabrication of these machines, it is necessary to consider some physical properties of the seeds (3, 4). The physical properties are also required for the design and evaluation of equipment and systems for their handling, processing, and storage (5). Processing techniques and proper handling of almond require accurate knowledge of the physical properties such as shape, size, porosity, surface area, bulk density (6). The size, shape, and physical dimensions of almond seeds are important in sizing, sorting, and other separation processes. The porosity is the fraction of the space in the bulk seeds which is not occupied by the seeds (7). Additionally, the porosity of fruits is the most important for packing. Bulk density and porosity affect the structural loads and are important parameters in designing drying and storing systems. Seed weight, seed volume, seed density and mean geometric diameters could be used to characterize the almond seed. Today, there are only a few data in the literature describing the physical and mechanical properties of almond and its kernel, some of them are pointed out in the following. For instance, Loghavi et al. (8) studied the physical and mechanical properties of almonds. In this study, the physical and mechanical properties of an Iranian almond variety (Prunus dulcis l. cv. 7Shahrood) in three forms of green, unshelled, and shelled kernels are measured. The properties measured included mass, moisture content, arithmetic, and geometric mean diameter, surface area, sphericity, shape index, bulk and true density, porosity, angle of repose, static coefficient of friction, and rolling angle. Green almond has the maximum moisture content, geometric and arithmetic mean diameters, surface area, and sphericity while shelled almond has the minimum value for these parameters. Shape index is

*Corresponding author: Department of Food Science and Technology, Roudehen Branch, Islamic Azad University, Roudehen, Iran.
E-mail address: Mokhtarian.mo@gmail.com (Mohsen Mokhtarian).

the highest in shelled almond and the lowest in green almond. True and bulk densities are the highest for the shelled and unshelled kernels and the lowest for the green and shelled kernels, respectively. Besides, Altuntas et al. (9) explained the mechanical and geometric properties of different almond cultivars. The average sphericity, volume, and surface area ranged from 60.5 to 71.1%; 3.52 to 3.81 cm^3 and 0.60 to 0.61 cm^2 for almond cultivars. The greatest and least rupture force of almond was obtained along the X and Z axes for each cultivar. The results indicated that the effects of compression along the axis and speed on the rupture force were highly dependent on almond cultivars. Selected mechanical properties were affected by geometric and mechanical parameters of almond cultivars. Aydin (10) studied some engineering properties of peanut fruit and kernels were evaluated as functions of moisture content. At the moisture content of 4.85% d.b. the average length, thickness, width, geometric mean diameter, sphericity, unit mass, and volume of peanut fruits were 44.53 mm, 15.71 mm, 16.68 mm, 23.00 mm, 51.60%, 2.16 g, and 5.17 cm^3, respectively. Corresponding values for kernel at the moisture content of 6.00% d.b. were 20.95 mm, 8.80 mm, 10.44 mm, 12.60 mm, 57.05%, 1.063 g, and 1.14 cm^3, respectively. Studies on re-wetted peanuts showed that the bulk density decreased from 243 to 184 kg/m^3, the true density, projected area, and terminal velocity increased from 424 to 545 kg/m^3, 4.88 to 6.85 $cm^{2,}$ and 7.25 to 7.93 m/s, respectively as the moisture content increased from 4.85% to 32.00% d.b.; for the kernel, the corresponding values changed from 581 to 539 kg/m^3, 989 to 1088 kg/m^3, 1.53 to 2.09 cm^2 and 7.48 to 8.06 m/s, respectively as the moisture content increased. Turkan et al. (11) measured the average length, width, and thickness of a Golkan 23-101 almond cultivar to be 36.60, 19.24, and 11.47 mm, respectively, and 31.10, 18.31, and 11.04 mm for Nanparil cultivar, respectively. Also, averages for mass, volume, geometric average, sphericity, and surface area for Golkan 23-101 cultivar were 3.02 g, 4.24 cm^3, 20.03 mm, 54%, and 12.61 cm^2, respectively, and for Nanparil cultivar were 1.72 g, 3.33 cm^3, 18.50 mm, 59%, and 12.80 cm^2, respectively. Furthermore, Aydin (12) scrutinized the mechanical and physical properties of a kind of almond that grows in Turkey. Average amounts for length, width, and thickness for almond were 25.49, 12.03, and 12.17 mm, respectively, and for the kernel were 21.19, 11.34, and 6.38, respectively. Also, averages for mass, volume, geometric average, and sphericity were 2.64 g, 2.61 cm^3, 18.13 mm, and 69.59% for almond, respectively, and for the kernel were 0.73 g, 0.82 cm^3, 11.42 mm, and 55.17%, respectively. Viswanathan et al. (13) found a linear decrease in true density, bulk density, and porosity of neem nut with an increase in moisture content in the range 7.6-21 % w.b. Artificial neural network (ANN) is a general non-linear model based on a simplified model of human brain function and this technique is particularly useful when a phenomenological model of a process is not available or would be too far complex. Artificial neural networks have already been applied to simulate processes such as fermentation (14), drying behavior of different food and agricultural materials such as carrot (15), ginseng (16), cassava and mango (17), sorption isotherms (18), and drying (19, 20), but there is no information about the application of artificial neural networks to forecast geometrical and gravimetrical properties (such as surface area, kernel density, seeds volume and seeds mass) of almond seeds. The aim of this research was the utilization of artificial biological neurons to forecast the geometrical and gravimetrical properties of almond for the first time.

2. Material and methods

2.1. Raw material preparation

In this research, almond (Mama'e variety) was purchase from a local market and it was transferred to the laboratory. The samples were cleaned in a cleaner air screen to remove foreign matter such as dust, dirt, stones, and chaff as well as blank, broken, and immature almond. The samples were broken and the kernels separated from the shell by hand and were packed in a hermetic container. The initial moisture content of the almond was determined by using the standard method (21) and was found to 4.33 % w.b.

2.2. Physical properties measurement

The samples of the desired moisture levels were prepared by adding calculated amounts of distilled water, thorough mixing, and then scaling in separate polyethylene bags. The samples were kept at 5ºC in a refrigerator for 7 days for moisture to distribute uniformly throughout the sample and mold growth prevention. Before starting the test, the required quantities of the almonds were allowed to warm up to ambient temperature (22, 23). The moisture content of the samples was determined after they attained equilibrium to ensure moisture to distribute uniformly throughout the sample. All the physical properties of almonds kernel were assessed at moisture levels of 4.33 to 35.8 % w.b. Those of higher moisture content was obtained by adding distilled water of mass given by the formula (Eq. 1):

$$Q = \frac{w_i(m_f - m_i)}{(100 - m_f)} \quad (1)$$

where, Q is mass of added water (g), w_i is the initial mass of sample (g), m_i is the percentage of initial moisture content (%w.b) and m_f is the percentage of final moisture content (%w.b).

To determine the average size of almond kernel, 100 almond were randomly selected. The axial dimension of almond kernel, namely, length (L), width (W), and thickness (T) were measured with a caliper (Vertex, M502) to an accuracy of 0.01 mm. The geometric mean diameter (D_g) of almond kernels was calculated by using the following relationship at each moisture level (24) (Eq. 2).

$$D_g = \sqrt[3]{L \times W \times T} \quad (2)$$

In the above equation, D_g is the geometric mean diameter (mm), L is length (mm), W is the width (mm) and T is the thickness (mm). To obtain the mass, each almond kernel was measured by using an electronic balance (Qhaus Scale Co. G160D, W. Germany) of 0.001 g sensitivity. Seed volume (V)

and seed surface area (S) were calculated using the formula stated by Jain and Bal (25) (Eqs. 3 and 4):

$$S = \frac{\pi B^2 L^2}{2L-B} \quad (3)$$

$$V = \frac{\pi B^2 L^2}{6(2L-B)} \quad (4)$$

In the above equations, $B=(WT)^{0.5}$, S is surface area (mm^2) and V is the volume (mm^3). In order to determine the bulk density (ρ_b), the almond kernels were filled into the calibrated bucket from a height of about 15 cm and excess seeds were removed by strike off the stick (24). The seeds were not compacted in any-way (Eq. 5).

$$\rho_b = \frac{m}{V_b} \quad (5)$$

In this equation, m is the bulk mass of almond kernels (g), V_b is the bulk volume (cm^3) and ρ_b is bulk density ($g.cm^{-3}$). The seed volume (V) and seed density (ρ_k), were determined using the liquid displacement method. Toluene (C_7H_8) was used instead of water because it is absorbed by seeds to a lesser extent. Also, its surface tension is low, so that it fills even shallow dips in seed and its dissolution power is low (23, 26).

2.3. Artificial neural networks

In this research, multilayer perceptron neural network (*MLP*) based on backpropagation network and radial basis function network (*RBFN*) were enforced to forecast physical properties of almond. The first model was a multilayer perceptron neural network. *MLP* network includes an input layer, a hidden layer, and an output layer (27). The second model was a radial basis function network. This form of the network had three layers: an input layer, a hidden layer with a non-linear *RBF* activation function, and a linear output layer. In this work, for *MLP* network used different activation functions namely the identity, the logarithmic sigmoid (*logsig*), and the hyperbolic tangent (*tanh*) and for RBF network used normalized radial basis function (*NRBF*) and ordinary radial basis function (*ORBF*). In both networks, length, width, and thickness were considered as input variables and surface area, volume, mass and kernel density were selected as output variables. Thus, ANN models were designed based on three neurons per input layer and four neurons per outlet layer (Fig. 1). In order to evaluate the network performance and the best-selected configuration were used from two criteria such as determination coefficient (R^2) and mean relative error (*MRE*). Also, the computer program SPSS version 17 (2011) was used in the design of the neural network.

$$R^2 = 1 - \left[\frac{\sum_{i=1}^{N}(U_{p,i}-U_{e,i})^2}{\sum_{i=1}^{N}(\overline{U}_{p,i}-U_{p,i})^2}\right] \quad (6)$$

$$MRE = \left(\frac{1}{N}\sum_{i=1}^{N}\frac{|U_{p,i}-U_{e,i}|}{U_{e,i}}\right) \times 100 \quad (7)$$

Where $U_{p,i}$ is predicted data, $U_{e,i}$ is experimental data, $\overline{U}_{p,i}$ is the average of experimental data and N is the number of observations.

3. 3. Results and discussion

In this study a combination of various layers and neurons with different activation functions (at hidden and outer layers) has used to modeling of multilayer perceptron network and radial basis function network. Here, the neural networks with one hidden layer, 2 to 50 neurons were selected randomly and the power of network determined at predicting the almond physical properties. To training the perceptron network, back propagation algorithm was used, and the momentum coefficient for all networks was 0.9 and the learning rate was 0.4. In order to identify a suitable learning epoch, one experimental network includes various neuron numbers (2 to 50 neuron) along with different epochs number were used.

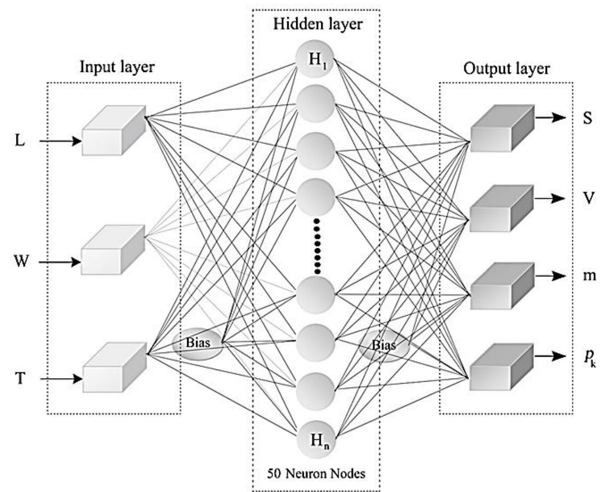

Fig. 1. Schematic of the neural network: length (L), width (W), thickness (T), seed surface area (S), seed volume (V), seed mass (m), and kernel density (ρk).

The results showed that the best learning epoch of 5000 has the best accuracy in predicting almond physical properties and also it prevents over-training of the network. The intent of optimizing the best learning epoch were achieved the lowest mean relative error. Determination of suitable learning epoch was based on trial and error method. As it is mentioned, in this study two different models of the artificial neural network were used along with different activation functions to predict the almond physical properties. Optimization results of multilayer perceptron network with *logsig-logsig*, *tanh-tanh*, *logsig-tanh*, *logsig-identity* and *tanh-identity* activation functions, along with different configurations are shown in Table 1. Investigation of obtained results for *MLP* with *logsig-logsig* activation function with one hidden layer has been shown, the configuration of 3-22-4 (i.e. network with 3 inputs, 22 neurons in the first hidden layer and 2 outputs) had the best result to predict almond physical properties. On the other hand, results of *MLP* network with *tanh-tanh* activation function showed that a neural network with the configuration of 3-34-4 had the best result in predicting almond physical properties. So that, this network could estimate the surface area, seed volume, seed mass, and kernel density with regression coefficients of

Table 1. The results of MLP network to forecast almond physical properties.

Activation functions	Parameters	SP*	No. of neurons												
			2	**6**	**10**	**14**	**18**	**22**	**26**	**30**	**34**	**38**	**42**	**46**	**50**
Log/ Log	Surface area	*MRE***	0.8919	0.994	1.2207	1.1457	1.0114	0.0981	0.6813	1.1041	1.2191	0.6774	0.4828	1.1358	1.1476
		R^2	0.481	0.459	0.385	0.339	0.431	0.903	0.652	0.411	0.397	0.664	0.741	0.362	0.339
	Volume	*MRE*	0.8774	0.9948	0.9943	1.0636	1.067	0.0937	0.6339	1.0338	1.0028	0.7575	0.5352	1.1401	1.1432
		R^2	0.595	0.532	0.532	0.439	0.421	0.909	0.679	0.476	0.498	0.637	0.729	0.375	0.361
	Mass	*MRE*	0.9591	1.0016	1.0388	1.0871	1.0202	0.1932	0.6002	0.9899	1.0158	0.4958	0.4294	1.0658	1.0778
		R^2	0.423	0.397	0.349	0.278	0.369	0.866	0.529	0.402	0.382	0.675	0.591	0.312	0.301
	Kernel density	*MRE*	0.972	0.9798	1.0688	1.1092	1.0513	0.1517	0.7372	1.035	1.0598	0.8118	0.445	1.1424	1.355
		R^2	0.503	0.503	0.418	0.387	0.462	0.868	0.646	0.487	0.455	0.591	0.742	0.31	0.361
Tanh/ Tanh	Surface area	*MRE*	0.8697	1.1914	1.4771	0.6089	1.9845	0.8469	0.5864	0.0499	0.0159	1.8665	1.6328	2.0691	0.9576
		R^2	0.477	0.379	0.346	0.579	0.259	0.493	0.64	0.949	0.983	0.273	0.309	0.223	0.412
	Volume	*MRE*	0.9178	1.1324	0.9559	0.682	1.7489	1.022	0.5824	0.0505	0.012	1.4214	1.9111	1.8935	1.0808
		R^2	0.429	0.301	0.408	0.502	0.267	0.372	0.651	0.947	0.986	0.281	0.245	0.245	0.341
	Mass	*MRE*	0.8785	1.1559	1.073	1.1024	1.8235	1.139	0.8118	0.0593	0.0163	2.405	1.8519	2.108	1.263
		R^2	0.443	0.344	0.385	0.379	0.286	0.175	0.498	0.947	0.981	0.213	0.285	0.248	0.308
	Kernel density	*MRE*	0.9526	1.1046	0.9245	0.9054	1.4531	1.2188	0.6313	0.0751	0.022	1.2183	1.3664	1.4483	0.6087
		R^2	0.327	0.302	0.358	0.397	0.222	0.339	0.589	0.903	0.982	0.287	0.252	0.231	0.601
Log/ Tanh	Surface area	*MRE*	1.0198	0.9458	0.8888	1.1722	1.0516	1.1789	1.25	0.6018	1.592	1.1658	0.0972	0.9837	1.1336
		R^2	0.355	0.394	0.448	0.301	0.352	0.301	0.256	0.678	0.206	0.316	0.927	0.372	0.322
	Volume	*MRE*	1.0162	0.9726	0.9584	1.1451	1.1206	1.1356	1.1964	0.7996	1.069	1.1653	0.0635	0.9882	1.2338
		R^2	0.351	0.421	0.437	0.271	0.306	0.294	0.233	0.542	0.322	0.246	0.944	0.384	0.203
	Mass	*MRE*	1.0101	0.9277	1.0428	1.0917	1.1131	1.0929	1.4225	0.6781	1.1264	1.1734	0.0985	0.9446	1.3002
		R^2	0.376	0.426	0.362	0.35	0.332	0.349	0.29	0.578	0.321	0.243	0.92	0.391	0.2
	Kernel density	MRE	1.0316	0.9433	0.6593	1.1515	0.9755	2.299	1.0043	0.6002	1.245	2.2398	0.0526	0.79	2.2548
		R^2	0.311	0.386	0.549	0.281	0.36	0.185	0.333	0.594	0.234	0.215	0.94	0.422	0.208
Log/ Identity	Surface area	MRE**	0.7846	1.0226	0.8324	1.1293	0.9106	0.6902	0.784	0.5553	1.19	1.1324	0.0331	0.8278	1.0583
		R2	0.497	0.426	0.478	0.38	0.441	0.723	0.52	0.798	0.32	0.376	0.965	0.491	0.414
	Volume	MRE	0.8066	1.3559	0.8781	1.1306	0.9143	0.7285	0.7642	0.7197	0.9934	1.1753	0.0354	0.8872	1.1155
		R2	0.451	0.203	0.391	0.242	0.341	0.546	0.491	0.612	0.301	0.211	0.968	0.382	0.26
	Mass	MRE	1.0824	1.0561	0.8644	1.025	0.9314	0.7431	0.6934	0.7156	0.9965	1.045	0.0402	0.7527	0.9598
		R2	0.371	0.389	0.551	0.415	0.472	0.699	0.781	0.71	0.438	0.405	0.958	0.637	0.459
	Kernel density	MRE	1.0745	1.2376	0.8583	1.2465	0.9761	0.5561	0.9952	0.6268	1.2798	1.3654	0.1466	0.8676	1.0394
		R2	0.419	0.39	0.583	0.387	0.47	0.743	0.456	0.629	0.37	0.351	0.848	0.551	0.432
Tanh/ Identity	Surface area	MRE	0.471	1.0636	1.1378	0.295	0.3089	0.749	0.4745	0.1914	0.0182	0.1089	1.1308	0.701	0.1552
		R2	0.684	0.415	0.365	0.726	0.701	0.476	0.651	0.826	0.983	0.941	0.395	0.518	0.873
	Volume	MRE	0.6934	1.0952	1.1391	0.3328	0.3852	0.8118	0.4952	0.2269	0.0164	0.0569	1.3748	0.6282	0.1686
		R2	0.623	0.489	0.412	0.779	0.722	0.582	0.667	0.804	0.98	0.945	0.391	0.682	0.863
	Mass	MRE	0.6022	1.0889	1.1389	0.372	0.3792	0.8283	0.5504	0.2391	0.0218	0.0652	1.6209	0.5965	0.1508
		R2	0.534	0.431	0.412	0.743	0.727	0.482	0.581	0.823	0.98	0.935	0.396	0.546	0.871
	Kernel density	MRE	1.3154	1.1504	1.1984	0.4791	0.5994	0.8624	0.6021	0.5532	0.0532	0.1521	1.4161	0.4922	0.2062
		R2	0.391	0.435	0.423	0.695	0.56	0.594	0.539	0.701	0.891	0.822	0.387	0.671	0.778
Log/ Identity	Surface area	MRE**	0.7846	1.0226	0.8324	1.1293	0.9106	0.6902	0.784	0.5553	1.19	1.1324	0.0331	0.8278	1.0583
		R2	0.497	0.426	0.478	0.38	0.441	0.723	0.52	0.798	0.32	0.376	0.965	0.491	0.414
	Volume	MRE	0.8066	1.3559	0.8781	1.1306	0.9143	0.7285	0.7642	0.7197	0.9934	1.1753	0.0354	0.8872	1.1155
		R2	0.451	0.203	0.391	0.242	0.341	0.546	0.491	0.612	0.301	0.211	0.968	0.382	0.26
	Mass	MRE	1.0824	1.0561	0.8644	1.025	0.9314	0.7431	0.6934	0.7156	0.9965	1.045	0.0402	0.7527	0.9598
		R2	0.371	0.389	0.551	0.415	0.472	0.699	0.781	0.71	0.438	0.405	0.958	0.637	0.459
	Kernel density	MRE	1.3154	1.1504	1.1984	0.4791	0.5994	0.8624	0.6021	0.5532	0.0532	0.1521	1.4161	0.4922	0.2062
		R2	0.391	0.435	0.423	0.695	0.56	0.594	0.539	0.701	0.891	0.822	0.387	0.671	0.778

*Statistical parameters; **Mean relative error.

0.983, 0.986, 0.981, and 0.982, respectively, whereas such network with *logsig-logsig* could predict the surface area, seed volume, seed mass and kernel density with a regression coefficient of 0.930, 0.909, 0.866, and 0.868, respectively. Thus, according to the results of both functions, it is suggested that *tanh-tanh* activation function have high capability to predict the almond physical properties than *logsig-logsig* activation function. The results of *MLP* network with *logsig-tanh* activation function showed that a neural network with 4-42-3 structure presented the best result for forecasting almond physical properties. The network estimates the surface area, seed volume, seed mass, and kernel density with a mean relative error of 0.0972, 0.0635, 0.985, and 0.0526, respectively. The results of this network present in Table 1. As it is observed, the results showed that such a network with the configuration of 42 neurons per hidden layer could predict the surface area, seed volume, seed, and kernel density with R^2 value of 0.927, 0.944, 0.920, and 0.940, respectively. A study of other configuration results for predicting the almond physical properties showed a low accuracy to predict almond physical properties. Thus, a nervous structure with 42 neurons in the hidden layer was selected as the best configuration (with *logsig-tanh* activation function) (Table 1). Also, the results of *MLP* network with *logsig-identity* activation function are present in Table 1. Application of this network to predict almond physical properties showed that a neural network with the configuration of 42 neurons per hidden layer showed better results than the other neurons. The results showed that other neurons had low accuracy for predicting the amount of almond physical properties. (Regression coefficients were between 0.203 to 0.798). On the other hand, the results of *MLP* network with *tanh*-identity activation function showed that this network with the lower amount of neurons (No. of 34) from *MLP* network with *logsig-identity* activation function, could predict the almond physical properties. R^2 value for *MLP* network with *tanh-identity* activation function about the prediction of surface area, seed volume, seed mass, and kernel density were 0.983, 0.980, 0.980 and 0.891, respectively. In comparison with *MLP* network with *logsig-identity* activation function has high capability to predicting almond physical properties (in this network, R^2 value for the surface area, seed volume, seed mass, and kernel density were 0.965, 0.968, 0.958, and 0.848, respectively). The results of the radial basis function network model along with normalized radial base function and ordinary radial base function are present in Table 2. As it observed from Table 2, radial base function network along with normalized radial with normalized radial base function showed that 3-46-4 configuration (i.e. network with 3 inputs, 46 neurons in the first hidden layer, and 4 outputs), provided the best result to predicting surface area, seed volume, seed mass, and kernel

Table 2. The results of RBF network to forecast almond physical properties.

Activation functions	Parameters	SP*	No. of neurons												
			2	6	10	14	18	22	26	30	34	38	42	46	50
NRBF	Surface area	*MRE***	0.4823	0.1929	0.15	0.1251	0.1046	0.061	0.0518	0.0461	0.0419	0.0432	0.0256	0.0224	0.0229
		R^2	0.514	0.801	0.846	0.871	0.892	0.936	0.944	0.95	0.954	0.952	0.972	0.976	0.975
	Volume	*MRE*	0.4823	0.1929	0.15	0.1251	0.1046	0.061	0.0518	0.0461	0.0419	0.0432	0.0256	0.0224	0.0229
		R^2	0.514	0.801	0.846	0.871	0.892	0.936	0.944	0.95	0.954	0.952	0.972	0.976	0.975
	Mass	*MRE*	0.5166	0.2211	0.1743	0.1351	0.1118	0.062	0.0517	0.046	0.0413	0.0429	0.0245	0.0209	0.0216
		R^2	0.481	0.774	0.823	0.861	0.885	0.936	0.945	0.95	0.954	0.952	0.974	0.977	0.976
	Kernel density	*MRE*	0.5785	0.3351	0.3215	0.225	0.2085	0.1871	0.1378	0.1226	0.1192	0.1205	0.0819	0.071	0.0718
		R^2	0.394	0.64	0.655	0.752	0.772	0.789	0.836	0.855	0.872	0.851	0.889	0.913	0.912
ORBF	Surface area	*MRE*	0.4832	0.205	0.1846	0.1676	0.1727	0.1175	0.108	0.0904	0.052	0.0387	0.0255	0.0228	0.0223
		R^2	0.512	0.789	0.811	0.827	0.825	0.88	0.889	0.905	0.942	0.959	0.974	0.977	0.977
	Volume	*MRE*	0.4832	0.205	0.1846	0.1676	0.1727	0.1175	0.108	0.0904	0.052	0.0387	0.0255	0.0228	0.0223
		R^2	0.512	0.789	0.811	0.827	0.825	0.88	0.889	0.905	0.942	0.959	0.974	0.977	0.977
	Mass	*MRE*	0.5209	0.2343	0.2078	0.1716	0.1766	0.1134	0.1026	0.0852	0.0473	0.0352	0.0245	0.0215	0.0209
		R^2	0.477	0.761	0.789	0.824	0.821	0.884	0.895	0.911	0.948	0.963	0.975	0.978	0.979
	Kernel density	*MRE*	0.561	0.3448	0.3599	0.268	0.2906	0.2665	0.1967	0.1789	0.161	0.141	0.0816	0.0716	0.0707
		R^2	0.404	0.632	0.627	0.722	0.701	0.719	0.782	0.801	0.816	0.849	0.918	0.928	0.929

*Statistical parameters; **Mean relative error.

Table 3. Compression of different model of ANNs.

Models	Activation function	Statistics parameters	Surface area	Seed volume	Seed mass	Kernel density
MLP	*Log/Log*	R^2	0.903	0.909	0.866	0.868
		MRE	0.0981	0.0937	0.1932	0.1517
		topology	3-22-4	3-22-4	3-22-4	3-22-4
	Tanh/Tanh	R^2	0.983	0.986	0.981	0.982
		MRE	0.0159	0.0120	0.0163	0.0220
		topology	3-34-4	3-34-4	3-34-4	3-34-4
	Log/Tanh	R^2	0.927	0.944	0.920	0.940
		MRE	0.0972	0.0635	0.0985	0.0526
		topology	3-42-4	3-42-4	3-42-4	3-42-4
	Tanh/Identity	R^2	0.983	0.980	0.980	0.891
		MRE	0.0182	0.0164	0.0218	0.0532
		topology	3-34-4	3-34-4	3-34-4	3-34-4
	Log/Identity	R^2	0.965	0.968	0.958	0.848
		MRE	0.0331	0.0354	0.0402	0.1466
		topology	3-42-4	3-42-4	3-42-4	3-42-4
RBFN	*NRBF*	R^2	0.976	0.976	0.977	0.913
		MRE	0.0224	0.0224	0.0209	0.0710
		topology	3-46-4	3-46-4	3-46-4	3-46-4
	ORBF	R^2	0.977	0.977	0.979	0.929
		MRE	0.0223	0.0223	0.0209	0.0707
		topology	3-50-4	3-50-4	3-50-4	3-50-4

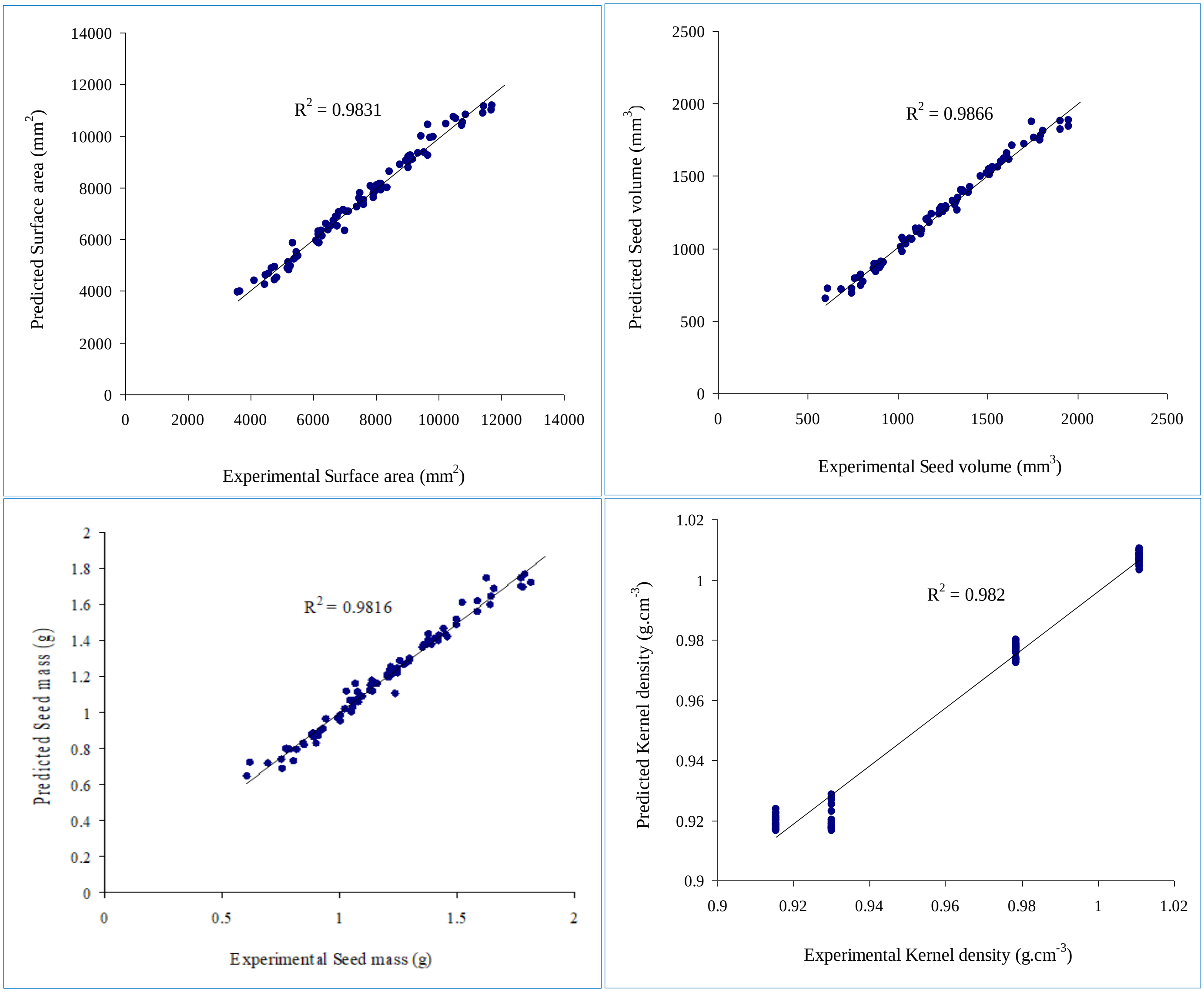

Fig 2. The amounts of predicted and experimental of physical properties by MLP network with tanh-tanh activation function.

density. The results of *RBF* network along with *ORBF* activation function showed that the best configuration at this network is 3-50-4. The comparison of the above-mentioned R^2 values in both cases showed that *RBF* network with *ORBF* provided the best results to predict the surface area, seed volume, seed mass, and kernel density. The values of R^2 to predict surface area, seed volume, seed mass, and kernel density were 0.977, 0.977, 0.979 and 0.929, respectively. Also the mean relative error values were 0.0223, 0.0223, 0.0209 and 0.0707, respectively. The comparison of various neural network models to determine the best model for predicting the almond physical properties are shown in Table 3. As can be seen, all models of the neural network had a high ability to predicting almond physical properties and R^2 value in all cases greater than 0.848. Nevertheless, the *MLP* networks along with *tanh-tanh* activation function with 34 neurons per hidden layer was selected as the best model due to having the maximum regression coefficient and minimum relative error to predicting the almond physical properties. The diagram of sensitivity analysis of predicted value by perceptron neural network along with *tanh-tanh* activation function against the experimental value for the best configuration of perceptron neural model (i.e. structure of 3-34-4) showed that data were randomly located around the regression line with R^2 value higher than 0.981. This could be a reason for carefully evaluating the neural networks to predicting almond physical properties (Fig. 2).

4. Conclusion

In this research, the physical properties of almond were anticipated by using an artificial neural approach. The results indicated that *MLP* network with *tanh-tanh* activation function was chosen as the best ANN model to forecasting almond physical properties as this network can be predicted surface area, seed volume, seed mass, and kernel density of almond with a regression coefficient of 0.983, 0.986, 0.981 and 0.982, respectively. Furthermore, in this paper surface area, seed volume, seed mass, and kernel density of almond were fitted by means of multilinear regression. The result is obtained as following equations. As can be seen, compression results of the best artificial neural model with multilinear regression model show that artificial neural model has been a high ability to forecasting the physical properties of almond.

Surface area:

$$S\ (mm^2) = -14465 - 0.34\ MC + 193\ L + 599\ W + 860\ T \qquad (R^2 = 0.979)$$

Seed volume:

$$V\ (mm^3) = -2411 - 0.056\ MC + 32.1\ L + 99.9\ W + 143\ T \qquad (R^2 = 0.961)$$

Seed mass:

$$m\ (g) = -2.12 - 0.00250\ MC + 0.0283\ L + 0.0943\ W + 0.132\ T \qquad (R^2 = 0.945)$$

Kernel density:

$$\rho_k\ (g/cm^3) = 1.10 - 0.00216\ MC - 0.00154\ L - 0.00089\ W - 0.00456\ T \qquad (R^2 = 0.791)$$

References

1. Abdallah A, Ahumada MH, Gradziel TM. Oil content and fatty acid composition of almond kernels from different genotypes and California production regions. *Journal of the American Society for Horticultural Science*. 1998;123:1029-33.
2. Kotwaliwale N, Brusewitz GH, Weckler PR. Physical characteristics of pecan components: effect of cultivar and relative humidity. *American Society of Agricultural Engineers*. 2004;47(1):227-31.
3. Aremu AK, Fowowe SO. Development and performance evaluation of a manually operated plantain-slicing machine. *Proceedings of the Nigerian Institution of Agricultural Engineers*. 2000;22:30-5.
4. Taser OF, Altuntas E, Ozgoz E. Physical properties of Hungarian and Common Vetch seeds. *Journal of Applied Science*. 2005;5(2):323-6.
5. Asoegwu SN, Maduike JO. Some physical properties and cracking energy of *Irvingea gabonensis* (ogbono) nuts. *Proceeding of the Nigerian Institution of Agricultural Engineers*. 1999;21:131-7.
6. Alabadan BA. Physical properties of selected biomaterials as related to their postharvest handling. *Proceeding of the Nigerian Society of Agricultural Engineers*. 1996;18:328-31.
7. Coskuner Y, Karababa E. Physical properties of coriander seeds (*Coriandrum sativum* L.). *Food Engineering*. 2007;80(2):408-16.
8. Loghavi M, Souri S, Khorsandi F. Physical and mechanical properties of almond (*Prunus dulcis* l. cv. 7Shahrood). *American Society of Agricultural and Biological Engineers*. 2011;doi:10.13031/2013.37425.
9. Altuntas E, Gercekcioglu R, Kaya C. Selected mechanical and geometric properties of different almond cultivars. *International Journal of Food Properties*. 2010;13: 282-93.
10. Aydin C. Some engineering properties of peanut and kernel. *Food Engineering*. 2007;79:810-6.
11. Turkan A, Polat R, Atay U. Comparison of mechanical properties of some selected almond cultivars with hard and soft shell under compression loading. *Food Engineering*. 2007;30:773-89.
12. Aydin C. Physical Properties of Almond Nut and Kernel. Food Engineering. 2003;60:315-20.
13. Viswanathan R, Palanisamy PT, Gothandapani L, Sreenarayanan VV. Some physical properties of Green Gram. *Journal of Agricultural Engineering*. 1996;63:19-26.
14. Latrille E, Corrieu G, Thibault J. pH prediction and final fermentation time determination in lactic acid batch fermentations. *Escape 2. Computers & Chemical Engineering*. 1993;17:423-8.
15. Erenturk S, Erenturk K. Comparison of genetic algorithm and neural network approaches for the drying process of carrot. *Food Engineering*. 2007;78:905-12.
16. Martynenko AI, Yang SX. Biologically inspired neural computation for ginseng drying rate. *Biosystems Engineering*. 2006;95(3):385-96.
17. Hernandez-Perez JA, Garcia-Alvarado MA, Trystram G, Heyd B. Neural networks for heat and mass transfer prediction during drying of cassava and mango. *Innovative Food Science and Emerging Technologies*. 2004;5:57-64.
18. Janjai S, Intawee P, Tohsing K, Mahayothee B, Bala BK. Neural network modeling of sorption isotherms of longan (*Dimocarpus longan* Lour.). *Computers and Electronics in Agriculture*. 2009;66:209-14.
19. Tavakolipour H, Mokhtarian M, Kalbasi-Ashtari A. Intelligent monitoring of zucchini drying process based on fuzzy expert engine and ANN. *Journal of Food Process Engineering*. 2014;37:474-81.
20. Tavakolipour H, Mokhtarian M. Neural network approaches for prediction of pistachio drying kinetics. International Journal of Food Engineering. 2012;8:3,doi:10.1515/1556-3758.2481.
21. AOAC. Official methods of analysis, Association of Official Analytical Chemists, Washington, DC. 1990.
22. Dehspande SD, Bal S, Ojha TP. Physical properties of soybean. Journal of Agricultural Engineering Research. 1993;56:89-98.
23. Aydin C. Physical properties of hazel nuts. *Biosystems Engineering*. 2002;82(3):297-303.
24. Mohsenin NN. Physical properties of plants and animal materials, Gordon and Breach Science Publishers, NW, New York, 1980.
25. Jain RK, Bal S. Properties of pearl millet. *Journal of Agricultural Engineering Research*. 1997;66:85-91.
26. Demir F, Dogan H, Ozcan M, Haciseferogullari H. Nutritional and physical properties of hackberry (*Celtis australis* L.). *Food Engineering*. 2002;54:241-7.
27. Wu CH, McLarty JW. Neural Networks and Genome Informatics. Elsevier Publishing Co. USA, 2000.